

# Gradient Index Metamaterial Based on Slot Elements

Oliver Paul<sup>1</sup>, Benjamin Reinhard<sup>1</sup>, Bernd Krolla<sup>1</sup>, René Beigang<sup>1,2</sup>, and Marco Rahm<sup>1,2,1</sup>

<sup>1</sup>*Department of Physics and Research Center OPTIMAS, University of Kaiserslautern, Germany*

<sup>2</sup>*Fraunhofer Institute for Physical Measurement Techniques IPM, Freiburg, Germany*

(Dated: November 5, 2018)

We present a gradient-index (GRIN) metamaterial based on an array of annular slots. The structure allows a large variation of the effective refractive index under normal-to-plane incidence and thus enables the construction of GRIN devices consisting of only a small number of functional layers. Using full-wave simulations, we demonstrate the annular slot concept by means of a 3-unit-cell thin GRIN lens for the terahertz (THz) range. In the presented realizations, we achieved an index contrast of  $\Delta n = 1.5$  resulting in a highly refractive lens suitable for focusing THz radiation to a spot size smaller than the wavelength.

In the last ten years, metamaterials have emerged to be powerful tools for the manipulation of light on the subwavelength scale. From the very first day of metamaterials, the scientific interest has been driven by the possibility of guiding light by tailoring the effective material parameters. In this respect, various concepts have been proposed, ranging from gradient index materials [1–3], to invisibility cloaks [4–7] and other transformation optical structures [8–12]. Most of the concepts have only been experimentally realized in the microwave regime where comparatively simple fabrication techniques allow a large freedom in the metamaterial design. However, when approaching higher frequencies as the THz or the optical regime, the experimental realization becomes more challenging since the standard fabrication methods, such as photo- or electron beam lithography, allow only the fabrication of planar structures with a very limited number of layers. In order to compensate the layer restriction in the high frequency range, it is therefore important to use metamaterials that provide a high refractive index contrast. However, most of the metamaterial structures are very lossy and allow only a moderate change of the refractive index within an acceptable transmission window. In particular, this is the case for resonant elements which are usually associated with high intrinsic losses. One possibility to create a non-resonant element is to choose the operation frequency well below the resonance frequency and, hence, operate in the non-resonant region of the structure. This approach has been applied in Ref. 2 – 4 where the achieved index contrast was reported to be in the range of  $\Delta n = 0.7–0.9$ . In this paper, we present an alternative approach for a non-resonant, polarization-independent structure which allows a very large variation of the refractive index of about  $\Delta n = 1.5$  with high transmission and reasonable bandwidth for practical applications.

The unit cell of the proposed metamaterial consists of a  $3\ \mu\text{m}$  wide annular slot within a square metal patch as shown in Fig. 1(a). The metal layer is embedded in a cubic dielectric matrix with an edge length of  $60\ \mu\text{m}$ . The radius of the annular slot was varied in order to alter the effective index of refraction. We analyzed the electromagnetic properties of the metamaterial by full-wave time-domain simulations (CST Microwave Studio). To consider a realistic model, the metal layer was implemented by  $200\ \text{nm}$  thick copper with an electric conductivity of  $\sigma = 5.8 \times 10^7\ \text{S/m}$ . For the dielectric matrix, we

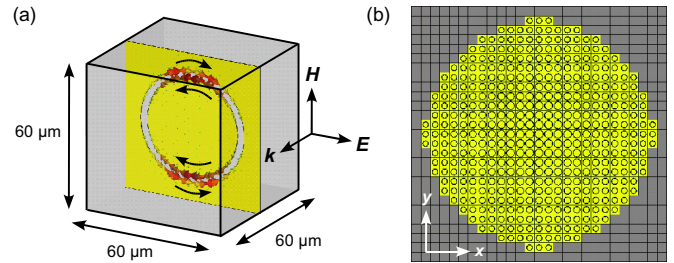


Fig. 1. (a) Unit cell of the annular slot structure with excited antisymmetric current mode. (b) Front view of the composed GRIN lens with a diameter of 25 unit cells.

used benzocyclobutene (BCB) with a relative permittivity of  $\epsilon = 2.67$  and a loss tangent of  $\tan \delta = 0.012$ .

The proposed GRIN metamaterial was composed of 3 layers of unit cells in the direction of propagation. The corresponding spectral transmission of a 3-layer-structure is presented in Fig. 2(b) for different values of the inner slot radius. The structure exhibits a broad transmission passband for frequencies between 1.2 THz and 1.9 THz with an amplitude transmission up to 85%. The enhanced transmission in the passband is related to the excitation of antisymmetric current modes at the inner and outer edge of the slot as indicated in Fig. 1(a). These antisymmetric modes exhibit a strongly reduced dipolar coupling to the external field leading to the observed high transmission.

The effective material parameters of the structure were determined by a retrieval algorithm as described in Ref. 13. The reliability of the effective medium description was corroborated by the observation that the retrieved parameters were independent of the number of unit cells in the direction of propagation, i.e. the thickness of the metamaterial slab. Furthermore, the real part of the retrieved index of refraction agreed with the values deduced from the phase advance of a propagating plane wave through the metamaterial slab. In Fig. 2(a), we present the retrieved refractive index  $n$  for varying values of the slot radius. Note that for frequencies above 1.5 THz, the half-wavelength inside the medium is smaller than the unit cell size (Bragg regime) and effective values are not expected to be reliable. The graphs show that the increasing transmission at the low frequency edge of the passband is related to a rapid increase of the refractive index from  $n \approx 0$  to values

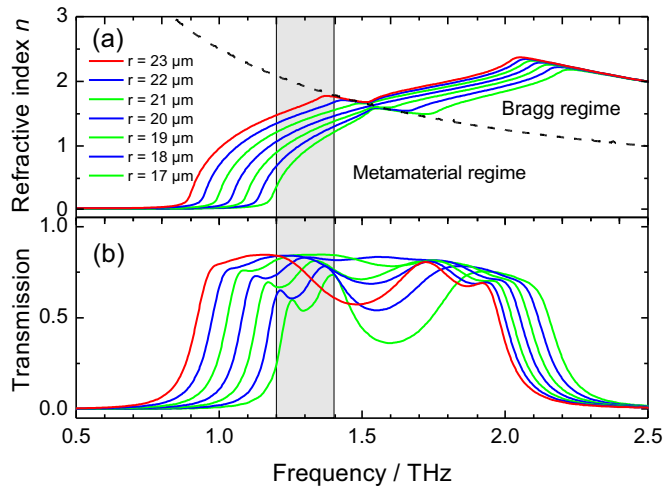


Fig. 2. (a) Real part of the effective index of refraction  $n$  for varying inner radius  $r$  of the slot. (b) Amplitude transmission for three unit cells in the direction of propagation. The spectral operation range of the GRIN lens is indicated by a grey box.

of about  $n \approx 1.6 - 1.8$ . This behavior is caused by a Drude-like response of the effective permittivity whereas the effective permeability is almost constant (see Fig. 3) implying the observed increase of  $n$  and of the transmission for frequencies above the plasma frequency  $\omega_p$ . The strong frequency dispersion of  $n$  is a key feature of the proposed GRIN lens since it allows a large variation of  $n$  within the passband by altering the slot radius. As seen from Fig. 2, the highest index contrast is achieved in the lower frequency range of the passband at about (1.2 – 1.4) THz with values up to  $\Delta n = 1.5$ . In this frequency interval, the ratio of the vacuum wavelength to the unit cell size is  $\lambda_0/a = 3.6 - 4.2$ .

In the following, we illustrate the optical properties of the proposed GRIN metamaterial by two exemplary realizations: A highly refractive lens with a very large index contrast of  $\Delta n = 1.51$  specified at a frequency of 1.2 THz (Lens 1) and a broadband lens applicable in the range of (1.2 – 1.4) THz (Lens 2). In each case, the GRIN lens was composed as a circular-shaped lens with a diameter of 25 unit cells, a thickness of 3 unit cells in the direction of propagation and was framed by a metallic aperture (see Fig. 1(b)). The incident THz wave was simulated by a linearly polarized plane wave and the overall calculation domain was terminated by open boundary conditions. The spatial refractive index profile of the GRIN lens was created by varying the inner radius  $r$  of the annular slot elements in dependence on their position within the lens. The appropriate relation between  $r$  and  $n$  was determined from the retrieved values of  $n$ . For example, Fig. 4(a) shows the dependence  $n(r)$  at the frequencies 1.2 THz, 1.3 THz, and 1.4 THz. For the broadband Lens 2, the radius was varied between 17  $\mu\text{m}$  and 22  $\mu\text{m}$ . In this interval, the relation between  $r$  and  $n$  is almost linear and, thus, the parabolic index profile was approx-

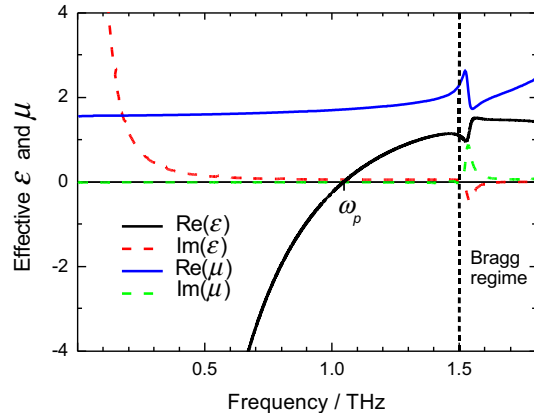


Fig. 3. Retrieved values for the effective permittivity  $\epsilon$  and permeability  $\mu$ , exemplarily shown for a slot element with an inner slot radius of  $r = 20 \mu\text{m}$ .

imated by a parabolic  $r$ -profile, according to

$$r(i, j) = (r_{\min} - r_{\max}) \frac{i^2 + j^2}{N^2} + r_{\max} \quad (1)$$

where  $i$  and  $j$  denote the cell indices in the  $x$ - and  $y$ -direction and  $N$  is the maximum cell index. For the highly refractive Lens 1, the inner radius of the slot elements was varied between 16  $\mu\text{m}$  and 24  $\mu\text{m}$ . Here, we optimized the accuracy of the index profile by determining a higher order fit for the inverse function  $r(n)$  at 1.2 THz and then setting  $r(i, j) = r(n(i, j))$  where  $n(i, j)$  describes a parabolic profile. The corresponding spatial refractive index profiles of both lenses are plotted in Fig. 4(b). It should be noted that the index profile of the broadband lens depends on the considered operation frequency due to the frequency dispersion of the refractive index.

In Fig. 5, we present the results of the 3D full wave simulations. Figs. 5 (a) – (d) show 2D plots of the electric field on selected planes for the highly refractive Lens 1. As expected, the GRIN lens provides the desired focusing functionality which is evidenced by uniformly curved phase fronts of the electric field in the  $y$ - $z$ -plane (Fig. 5(a)) and the high intensity at the focus (Fig. 5(d)). Moreover, the rotational symmetry of the field distribu-

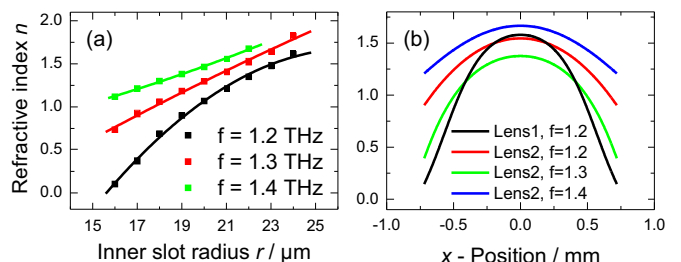


Fig. 4. (a) Retrieved values of the effective index of refraction  $n$  in dependence of the inner radius  $r$  of the annular slot at three different frequencies. (b) Spatial index profiles of the proposed highly refractive Lens 1 and of the broadband Lens 2 at three different frequencies in units of THz.

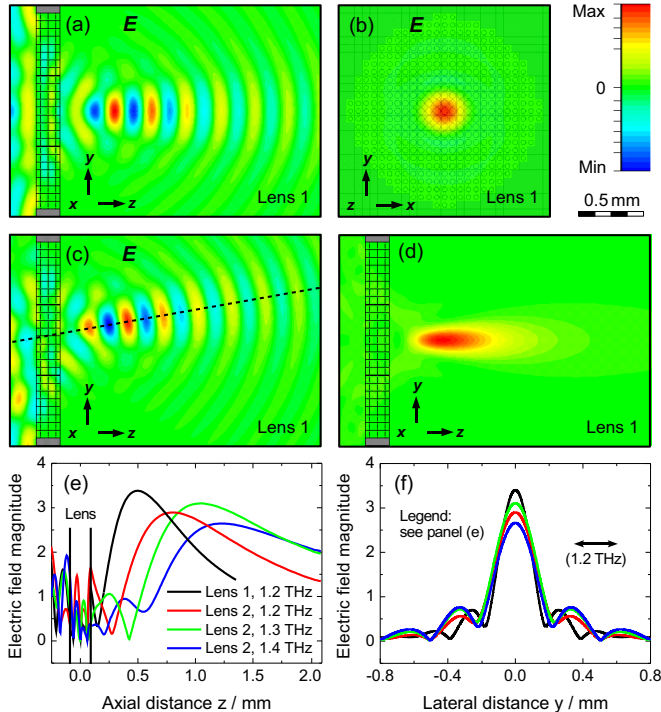


Fig. 5. Results of the full wave simulations of the highly refractive lens (Lens 1) and the broadband lens (Lens 2) for an  $x$ -polarized THz wave incident from the left. (a)  $x$ -component of the electric field at 1.2 THz in the  $y$ - $z$ -plane and (b) in the focal plane for normal incidence (with visible lens contours indicated in the background). (c) Same as (a) but for an incidence angle of  $\alpha = 11^\circ$ . (d) Time-averaged intensity in the  $y$ - $z$ -plane. (e) Magnitude of the electric field relative to the magnitude of the incident wave along the  $z$ -axis and (f) along the  $y$ -axis at the focus plane.

tion in the focal plane shown in Fig. 5(b) indicates that the focusing effect of the GRIN metamaterial is not sensitive to the polarization of the incident field. Furthermore, the focusing capabilities are maintained for oblique incidence. This is demonstrated in Fig. 5(c) for an incident wave at an angle of incidence of  $\alpha = 11^\circ$ . Obviously, the achieved spot size and focal length are almost identical to those for normal incidence (this holds for both TE and TM-polarized waves).

For a quantitative analysis of the proposed GRIN lenses, we evaluated the magnitude of the electric field along the  $z$ -axis as well as along the  $y$ -direction at the focal plane for both lens configurations. The obtained

axial and transverse beam profiles, normalized to the magnitude of the incident THz wave, are presented in Figs. 5(e) and 5(f). The graphs show that the proposed broadband lens (Lens 2) provides the desired focusing effect in the entire spectral range of (1.2 – 1.4) THz. However, as can be seen from Fig. 5(e), the frequency dependence of the refractive index  $n$  results in a noticeable chromatic aberration. In particular, the focal length ( $z$ -position where the field magnitude is maximal), increases from 0.8 mm at 1.2 THz to 1.2 mm at 1.4 THz. The increase of the focal length for higher frequencies agrees with the lowered curvature of the index profile shown in Fig. 4(b). The achieved focal spot diameters of both lenses are in the order of the wavelength of the incident THz wave (see Fig. 5(f)). As expected, the smallest spot size was achieved for the highly refractive Lens 1. According to the common definition of the spot diameter as the FWHM width of the intensity, the achieved spot diameter for Lens 1 was 170  $\mu\text{m}$  and, thus, was smaller than the wavelength of the incident THz wave,  $\lambda = 250 \mu\text{m}$ . Consequently, Lens 1 also produces the highest intensity in the focus. As seen from Fig. 5(e), the amplitude of the electric field at the focus is increased by a factor of 3.4 corresponding to an intensity enhancement of more than an order of magnitude.

In conclusion, we have analyzed and discussed an array of annular slots as a non-resonant, low-loss gradient index metamaterial. The structure provides a large achievable index contrast up to  $\Delta n = 1.5$  and a sufficient bandwidth for practical applications. The appropriateness of the design concept was demonstrated for the examples of a highly refractive lens and a broadband lens operating in the range of (1.2 – 1.4) THz, both consisting of only 3 layers of unit cells. The proposed lenses operate irrespectively of the polarization of the incident wave and are insensitive to the angle of incidence. Furthermore, we showed that the highly refractive lens is applicable to focus THz radiation to a spot size smaller than the wavelength of the incident wave where the THz intensity in the focus was increased by more than one order of magnitude. The planar geometry and the small number of necessary functional layers allow the fabrication of such metamaterials by standard multilayer BCB lithography techniques as described in Ref. 14. That way, the proposed design concept is especially advantageous for the development of tailored optical components for the THz technology. [13, 14]

[1] D. R. Smith, D. C. Vier, N. Kroll, and S. Schultz, “Direct calculation of permeability and permittivity for a left-handed metamaterial,” *Appl. Phys. Lett.* **77**, 2246–2248 (2000).  
 [2] R. Liu, Q. Cheng, J. Y. Chin, J. J. Mock, T. J. Cui, and D. R. Smith, “Broadband gradient index microwave quasi-optical elements based on non-resonant metamaterials,” *Opt. Express* **17**, 21,030–21,041 (2009).  
 [3] Q. Cheng, H. F. Ma, and T. J. Cui, “Broadband planar Luneburg lens based on complementary metamaterials,” *App. Phys. Lett.* **95**, 181,901 (2009).

[4] R. Liu, C. Ji, J. J. Mock, J. Y. Chin, T. J. Cui, and D. R. Smith, “Broadband Ground-Plane Cloak,” *Science* **323**, 366 (2009).  
 [5] W. Cai, U. K. Chettiar, A. V. Kildishev, and V. M. Shalaev, “Optical cloaking with metamaterials,” *Nature Photon.* **1**, 224 – 227 (2007).  
 [6] Z. Ruan, M. Yan, C. W. Neff, and M. Qiu, “Ideal Cylindrical Cloak: Perfect but Sensitive to Tiny Perturbations,” *Phys. Rev. Lett.* **99**, 113,903 (2007).  
 [7] J. Li and J. B. Pendry, “Hiding under the Carpet: A New Strategy for Cloaking,” *Phys. Rev. Lett.* **101**, 203,901

- (2008).
- [8] U. Leonhardt, “Optical Conformal Mapping,” *Science* **312**, 1777–1780 (2006).
- [9] J. B. Pendry, D. Schurig, and D. R. Smith, “Controlling Electromagnetic Fields,” *Science* **312**, 1780–1782 (2006).
- [10] D. Schurig, J. B. Pendry, and D. R. Smith, “Transformation-designed optical elements,” *Opt. Express* **15**, 14,772 (2007).
- [11] M. Rahm, S. A. Cummer, D. Schurig, J. B. Pendry, and D. R. Smith, “Optical Design of Reflectionless Complex Media by Finite Embedded Coordinate Transformations,” *Phys. Rev. Lett.* **100**, 063,903 (2008).
- [12] N. Kundtz and D. R. Smith, “Extreme-angle broadband metamaterial lens,” *Nat. Mater.* **9**, 129132 (2010).
- [13] X. Chen, T. M. Grzegorzczuk, B.-I. Wu, J. Pacheco, Jr., and J. A. Kong, “Robust method to retrieve the constitutive effective parameters of metamaterials,” *Phys. Rev. E* **70**, 016,608 (2004).
- [14] O. Paul, C. Imhof, B. Reinhard, R. Zengerle, and R. Beigang, “Negative index bulk metamaterial at terahertz frequencies,” *Opt. Express* **16**(9), 6736–6744 (2008).